

148. 2D-NMR Conformational Studies of Chiral Functionalized Ferrocenylphosphine Ligands for the Gold(I)-Catalyzed Aldol Reaction

by Antonio Togni*

Central Research Laboratories, Ciba-Geigy AG, Postfach, CH-4002 Basel

and Ruth E. Blumer and Paul S. Pregosin*

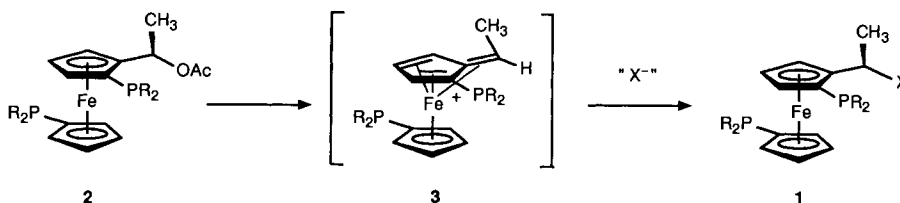
Laboratorium für anorganische Chemie, Universitätstrasse 6, ETH-Zentrum, CH-8092 Zürich

(24.VI.91)

The conformations in solution of six selected chiral 1,1'-bis(diphenylphosphino)ferrocenyl ligands bearing functionalized side chains, the diastereoisomers **4** and **5** and **6-9**, have been elucidated by 2D-NMR methods (COSY, TOCSY, NOESY, and ^1H , ^{31}P and ^1H , ^{13}C correlations). The possible relationship between the preferred conformation and the stereoselectivity observed in the gold(I)-catalyzed asymmetric aldol condensation in the presence of these ligands is discussed.

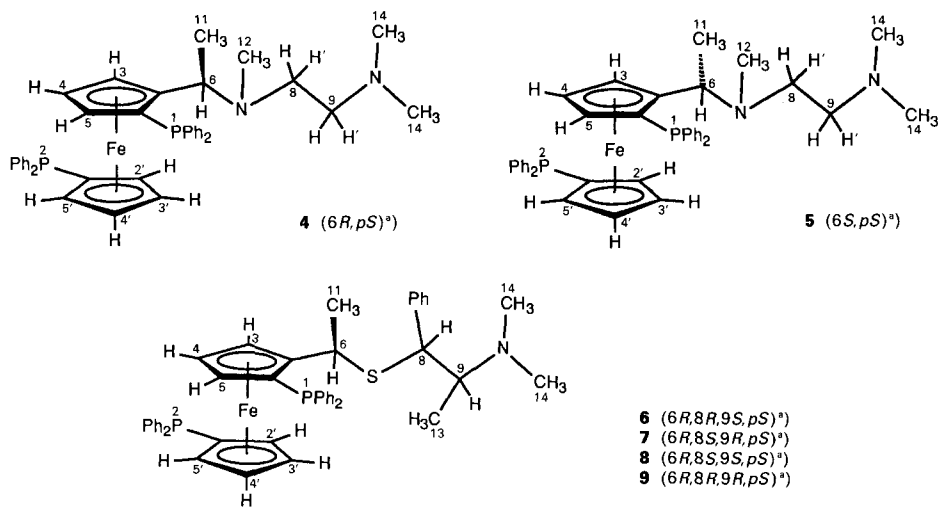
1. Introduction. – Chiral chelating ferrocenylphosphine ligands of type **1** have been used in a number of transition-metal-catalyzed reactions [1–3]. Their most important and unique features are: 1) they contain two (or more) chirotopic units [4], *i.e.* the ‘upper’¹⁾ cyclopentadienyl ring and the C-atom attached to it (additional centers of chirality can be introduced *via* the substituent X, *vide infra*), and 2) the presence of a heteroatom-containing substituent X which plays a crucial role in their catalytic reactions. Further, the nature of X can be adjusted to fulfill specific functional requirements [5]. The stereospecific introduction of the entity X, which occurs strictly with retention of configuration, rests upon the peculiar substitution chemistry of the 1-(ferrocenyl)ethyl acetate derivative **2**. This is connected with the intermediacy of the cationic, stabilized species **3** [6–8] (see *Scheme*). The Me substituent at C(α) of the aliphatic side chain plays a prominent role in the stereospecific chemistry of these compounds, and, as we will see, it is also responsible for some of their most important spectroscopic features.

Scheme. General Pathway for the Synthesis of Ferrocenylphosphines Containing a Functionalized Side Chain X. Bonding to the 1-(ferrocenyl)ethyl unit by a heteroatom (generally N).



¹⁾ In accordance with the usual representation of these compounds, we will refer to the disubstituted cyclopentadienyl ring as the ‘upper’ Cp and to the monosubstituted one as the ‘lower’ Cp.

One of the most elegant and successful applications of this type of ligand concerns the gold(I)-catalyzed condensation of aldehydes with isocyanacetates forming dihydrooxazoles (= 2-oxazolines) in high optical yields, as originally reported by *Hayashi and Ito* [9]. As part of an extended program devoted to asymmetric catalysis, mechanistic and stereochemical studies of this reaction have previously been undertaken [10–16]. From a phenomenological point of view, most interesting is the observation that diastereoisomeric ligands displaying different combinations of absolute configurations of the planar and central chiralities give rise to drastically diverging stereoselectivities. These studies lead to the notion of the *internal cooperativity of chirality* [11] [17], similar in concept to the principle of double stereodifferentiation described by *Masamune et al.* [18]. Thus, the ligands (*R,S*)-**4** and (*S,S*)-**5** gave the most striking results, leading to the formation of 4,5-disubstituted (*4S,5R*)- and (*4R,5S*)-dihydrooxazoles in 91 and 41% e.e., respectively [11]. This indicates that these two products arise from a matched and a mismatched diastereoisomeric form of the ligands, respectively. Furthermore, the four S-containing ligands **6–9**, exhibiting 1,2-disubstitution between the heteroatoms of the side chain, also showed large effects upon selectivity, depending on the specific combination of the absolute configurations [12]. Thus, **6** and **9** gave very low selectivities (ranging from 13 to 22% e.e. for both diastereoisomeric dihydrooxazoles), whereas **7** furnished both isomeric products in relatively high optical yields. Finally, **8** was found to be very similar to **4**, in terms of selectivity.



^{a)} Arbitrary numbering scheme; *p* refers to planar chirality.

We previously postulated that the observed differences in stereoselectivity using diastereoisomeric ligands is to be interpreted in terms of *different preferred time-averaged conformations* [10], in particular of the side chain, induced by a specific combination of chirotopic segments. A spectroscopic study of the conformation of Au^I complexes containing the ligands **4–9** under conditions relevant to catalysis (*i.e.* at *ca.* room temperature) is precluded by the highly dynamic nature of such complexes. To our knowledge, the

solid-state structure of $[(\text{AuCl})_3(\mathbf{4})_2]$ [15] represents the only known molecular structure of an Au^{I} complex containing ligand **4**. It is not apparent that the conformation of the side chain of the ligand is influenced in any relevant manner by the presence of coordinated AuCl units [15].

In earlier studies, we have reported on the utility of 2D ^1H -NOESY measurements for defining the nature of the chiral pocket of several selected catalysts, *i.e.* how and where the ligand interacts with a prochiral substrate [19] [20]. The premise upon which we based our work is straightforward: parts of the chiral ligand must intrude either into the coordination sphere or interact with the substrate. Consequently, we should be able to detect nuclear *Overhauser* effects (NOE's) between those molecular sections which develop close contacts. In connection with the observed large effects of *cooperativity* (*noncooperativity*) of *chirality* shown by the ligands **4–9**², we considered it worthwhile to develop a more detailed understanding of their structure in solution. It still remains a matter of speculation as to whether their conformational characteristics may also be assumed for the coordinated ligands in the transition state of the catalytic reaction. Assuming we could determine their conformation in solution, the crucial question is: does one find a correlation between the preferred time-averaged conformation of the ligands and the selectivity obtained in their catalytic reactions? Further, is it possible to learn which conformation the 'ideal' ligand should have?

We describe here detailed ^1H -, ^{31}P -, and ^{13}C -NMR studies on the six ligands **4–9** and specifically *a*) the configurational relationship of the stereogenic center C(6) to the ferrocenyl moiety and *b*) to the other chirotopic segment of the side chain, and *c*) the structural relationship of the different stereogenic centers C(8) and C(9) to one another². Low-temperature NMR studies of a catalytic system containing ligand **4** coordinated either to Au^{I} or Ag^{I} , and specifically addressing the participation of the pendant Me_2N group and its central role in the formation of the coordinated enolate have been recently reported by *Hayashi* and *Ito* [21].

2. Results and Discussion. – 2.1. *Assignment of the ^1H -NMR Spectra.* Given the moderate complexity of the molecules as well as the necessity for unequivocally³) assigning the cyclopentadienyl (Cp) resonances, the analysis customarily begins with COSY (or TOCSY) and 2D ^{31}P , ^1H -correlation measurements. The latter is especially useful in the assignment of both the ^{31}P -NMR spectra (which for this class of ligands typically appears as 2 broad *s*) and certain segments of the ^1H -NMR spectra. A typical example is shown in *Fig. 1*. Since P(2) is coupled to 2 H_c of Cp and P(1) only to 1 H_e , the ^{31}P assignments are immediately obvious.

The relayed ^1H , ^1H -COSY spectrum of **7** clearly indicates the three-spin and four-spin systems of the 'upper' and 'lower' Cp ring, respectively (*Fig. 2*, columns *c* and *d* (and also *g*), resp.). Since $\text{H}-\text{C}(4)$ is only coupled to $\text{H}-\text{C}(3)$ and $\text{H}-\text{C}(5)$, it is easily recognized. $\text{H}-\text{C}(5)$ appears at relatively high field as a consequence of the proximate diphenylphosphino group. Together with the COSY and NOESY data, it is now possible to identify all

²) The six compounds **4–9** have acetate **2** as common precursor; for an assignment of the absolute configuration of the planar chirality of **2** and its derivatives, see [6] [8]; the absolute configurations of the stereogenic centers in ligands **6–9** have been assigned elsewhere [12]. Throughout this work, the arbitrary numbering given in the *Formulae 4–9* is used; moreover, *p* refers to planar chirality.

³) Despite the various 1D and 2D methodologies combined with an 11.7 Tesla B_0 magnetic field, there are sometimes overlapping signals which cannot be unequivocally assigned.

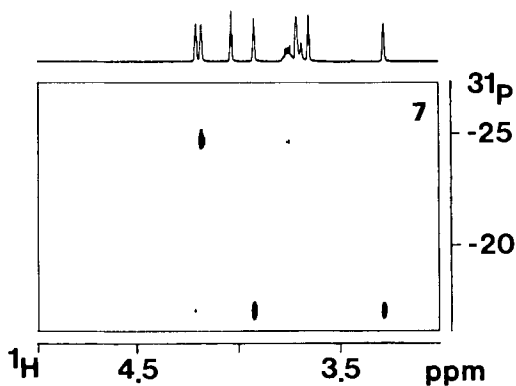
^{31}P , ^1H -Correlation

Fig. 1. Section of the 2D inverse ^{31}P , ^1H correlation spectrum (CDCl_3 , 500.13 MHz) of **7**. The only correlations from P(1) to one and from P(2) to two Cp protons are shown.

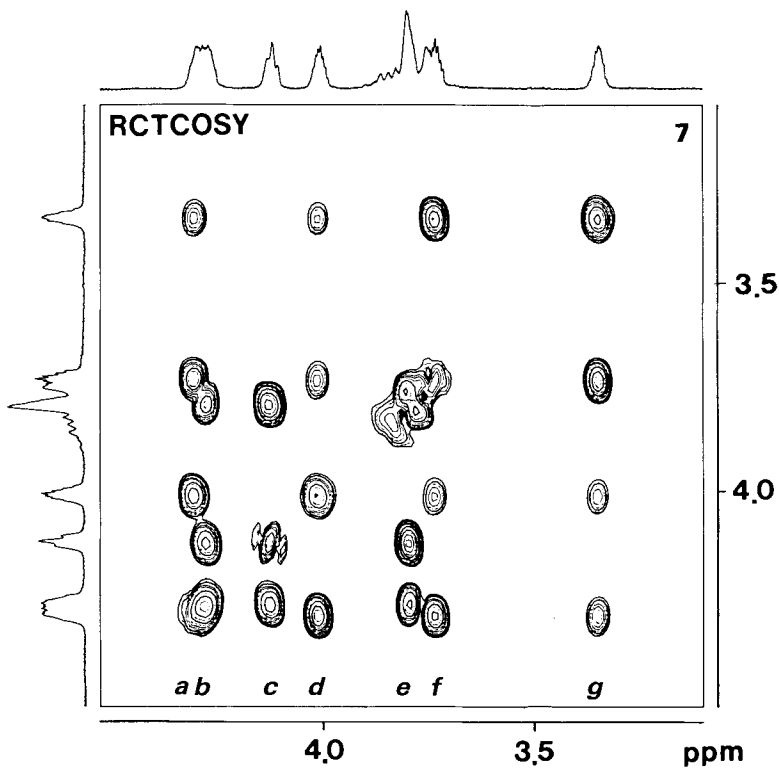


Fig. 2. Section of the ^1H -relayed COSY spectrum (CDCl_3 , 250 MHz) of **7**. The rows and columns clearly reveal the total number of spins involved in each spin system.

Cp resonances. With this knowledge, one can proceed to assign key aspects of the ^{13}C -NMR spectra, partially *via* DEPT and known empiricisms and partly *via* ^1H , ^{13}C correlations, using the data obtained as described above. *Tables 1–3* give selected ^1H -, ^{13}C -, and ^{31}P -NMR data for the six ligands **4–9** (some of the previous assignments were tentative).

Having made the ^1H -NMR assignments, several points are worth noting. For the diastereoisomers **4** and **5**, the chemical shift of $\text{CH}_3(11)$ (1.16 and 1.30 ppm, resp.) is the result of a deshielding P lone-pair effect [22] which is more pronounced in the (*S,S*)-isomer **5**. This suggests that the $\text{Ph}_2\text{P}(1)$ moiety has the Ph groups directed away from the aliphatic side chain. The same interpretation in terms of lone-pair deshielding applies to $\text{H}-\text{C}(6)$ of **4** and **5** (4.16 and 3.70 ppm, resp.). The large chemical-shift difference of the $\text{CH}_3(12)\text{N}$ signal of **4** and **5** (1.70 and 2.18 ppm, resp.) suggests somewhat different positions for the side chain in these diastereoisomers. We will refer to this point in *Chapt. 2.2*.

For the diastereoisomers **6–9** there are pronounced pair-wise changes, *e.g.* **6** and **9** are similar, as are **7** and **8**, and this behavior reflects the change in absolute configuration at C(8) (see *Table 1*). The $\text{CH}_3(13)$ signal of **6** is somewhat downfield by 0.1–0.2 ppm, presumably due to its relatively unique position.

2.2. NOESY Results. Since all ligands studied have the same absolute configuration at the 'upper' Cp ring (*S*), the molecular conformations are mainly discussed by viewing the complexes along the C(6)–C(2) axis. The preferred conformations of compounds **4** and **5** at this central unit C(2)–C(6) and of **6–9** at the C(8)–C(9) bond are deduced essentially from NOESY spectra and shown in *Fig. 3*.

There are several possible ways in which $\text{H}-\text{C}(6)$ and $\text{CH}_3(11)$ of **4** and **5** might sit with respect to the ferrocene moiety. The NOESY spectrum of **5** reveals a strong cross-peak due to $\text{H}-\text{C}(6)$ interacting with $\text{H}-\text{C}(3)$

Table 1. Selected ^1H -NMR Chemical Shifts [ppm] of **4–9**²⁾

	4 ^{a)}	5 ^{a)}	6 ^{b)}	7 ^{b)}	8 ^{b)}	9 ^{b)}
$\text{H}-\text{C}(3)$	4.36	4.39	4.32	4.18	4.24	4.32
$\text{H}-\text{C}(4)$	4.05	4.10	4.03	4.03	4.09	3.94
$\text{H}-\text{C}(5)$	3.64	3.51	3.62	3.71	3.83	3.51
$\text{H}-\text{C}(2')$	4.06	4.24	3.99	3.92	3.95	3.96
$\text{H}-\text{C}(3')$	4.36 ^{c)}	4.44	4.23	4.20	4.20	4.19
$\text{H}-\text{C}(4')$	3.97	4.02	3.71	3.65	3.59	3.66
$\text{H}-\text{C}(5')$	3.51	3.44	3.38	3.27	3.27	3.34
$\text{H}-\text{C}(6)$	4.16	3.70	3.49	3.75	3.71	3.21
$\text{H}-\text{C}(8)$	1.60	2.29 ^{d)}	4.00	3.69	3.89	3.73
$\text{H}'-\text{C}(8)$	1.69	^{d)}	–	–	–	–
$\text{H}-\text{C}(9)$	2.25	2.34 ^{d)}	2.37	2.57	2.77	2.42
$\text{H}'-\text{C}(9)$	2.43	^{d)}	–	–	–	–
$\text{CH}_3(11)$	1.16	1.30	1.42	1.03	1.13	1.39
$\text{CH}_3(12)$	1.70	2.18	–	–	–	–
$\text{CH}_3(13)$	–	–	0.68	0.39	0.49	0.43
$2\text{CH}_3(14)$	2.05	2.15	2.11	1.80	1.81	2.08

^{a)} 500.13 MHz, CDCl_3 .

^{b)} 200.13 MHz, CDCl_3 .

^{c)} Signal overlapping with that of $\text{H}-\text{C}(3)$.

^{d)} The 2 $\text{H}-\text{C}(8)$ and 2 $\text{H}-\text{C}(9)$ give 2 partially overlapping *m* which cannot be unequivocally assigned.

Table 2. Selected ^{13}C - a) and ^{31}P -NMR b) Chemical Shifts [ppm] of **4–9** c)

	4	5	6	7	8	9
C(1) or C(1')	76.90	75.10	c)	74.94	76.19	c)
C(1') or C(1)	77.55	76.65	c)	76.96	77.25	c)
C(2)	98.55	98.20	c)	101.23	101.74	c)
C(3)	72.14	72.71	c)	72.74	70.21	c)
C(4)	71.13	71.70	c)	72.27	71.56	c)
C(5)	73.45	73.19	c)	70.80	71.93	c)
C(2')	76.03	76.01	c)	75.89	75.33	c)
C(3')	74.82	74.89	c)	74.37	74.19	c)
C(4')	73.75	73.70	c)	73.35	72.56	c)
C(5')	73.50	73.27	c)	73.59	72.84	c)
C(6)	58.29	59.29	37.1	39.20	38.82	34.9
C(8)	58.20	57.54	55.8	56.35	56.11	54.8
C(9)	52.64	52.01	64.1	63.92	64.08	63.9
C(11)	9.81	16.50	23.2	23.61	23.26	21.9
C(12)	35.44	38.80	–	–	–	–
C(13)	–	–	8.6	10.73	8.61	8.5
C(14)	46.38	45.49	40.1	39.17	40.04	39.9
P(1)	–21.37	–23.49	–24.91	–24.82	–24.86	–24.17
P(2)	–17.01	–16.96	–17.19	–17.15	–17.14	–17.05

a) The ^{13}C -NMR spectra were obtained at 125.75 MHz for compounds **4**, **5**, **7**, and **8** and at 50.32 MHz for **6** and **9**.

b) All spectra obtained at 81.02 MHz.

c) Not assigned.

Table 3. Selected Coupling Constants [Hz] of **4–9** 2)

	4	5	6	7	8	9
$^3J(H-C(6),CH_3(11))$	6.7	7.0	6.5	7.0	7.0	6.5
$^4J(H-C(6),P(1))^a$	3–4	1–2	3–4	3–4	3–4	3–4
$^3J(H-C(8),H-C(9))$	–	–	6.5	8.8	9.2	10.0
$^3J(H-C(9),CH_3(13))$	–	–	6.5	6.7	6.4	6.5
$^4J(C(11),P(1))$	11.6	0	11.8	12.1	11.9	12.2

a) Because of the coupling with $CH_3(11)$, $^4J(H-C(6), P(1))$ is not well resolved.

(Fig. 4 cross-peak A) which is absent in the spectra of all other ligands. We conclude that this NOE arises from a conformation in which $H-C(6)$ and $H-C(3)$ are in a pseudo-*cis*-orientation. Reversal of the absolute configuration at C(6) leads to a pseudo-*trans*-arrangement of these two protons such that the NOE almost vanishes. Also apparent for **5** are modest NOE's arising from the interaction of $CH_3(11)$ with $H-C(3)$ (Fig. 4, cross-peak B), as well as with $H-C(2')$ and $H-C(3')$. This implies that $CH_3(11)$ lies below the Cp ring plane. Thus, $CH_3(11)$ avoids the large Ph_2P substituent and the N side chain is above the Cp ring. As a consequence of this conformation, a weak NOE between $CH_3(12)$ and $H-C(3)$ is also observed (this NOE is much weaker in **4**). There are weak cross-peaks from $H-C(6)$ to the Cp protons of the lower ring of **5**, suggesting that $H-C(6)$ may be slightly below the Cp plane, but there is no contact of $H-C(6)$ with the Ph_2P moiety. For ligand **4**, the significant $H-C(6),H-C(3)$ NOE is markedly reduced, whereas the interaction $CH_3(11),H-C(3)$ is very strong. Presumably, this stems from a conformation in which $H-C(6)$ is now facing the Ph_2P group and $CH_3(11)$ is remote from the latter, but still below the Cp plane. This is supported by the chemical-shift change mentioned above and an increase of $^4J(H-C(6),P(1))$ from ca. 1–2 Hz for **5** to ca. 3–4 Hz for **4**, in accordance with P lone-pair effects on four-bond spin-spin coupling constants [22].

In the ligands **6–9**, we find the same pattern of NOE's as in **4** ($H-C(3),CH_3(11)$ strong, $H-C(3),H-C(6)$ essentially zero, $J(P,H)$ ca. 3–4 Hz) and take this as characteristic for the absolute configuration (*6R,pS*). Apart

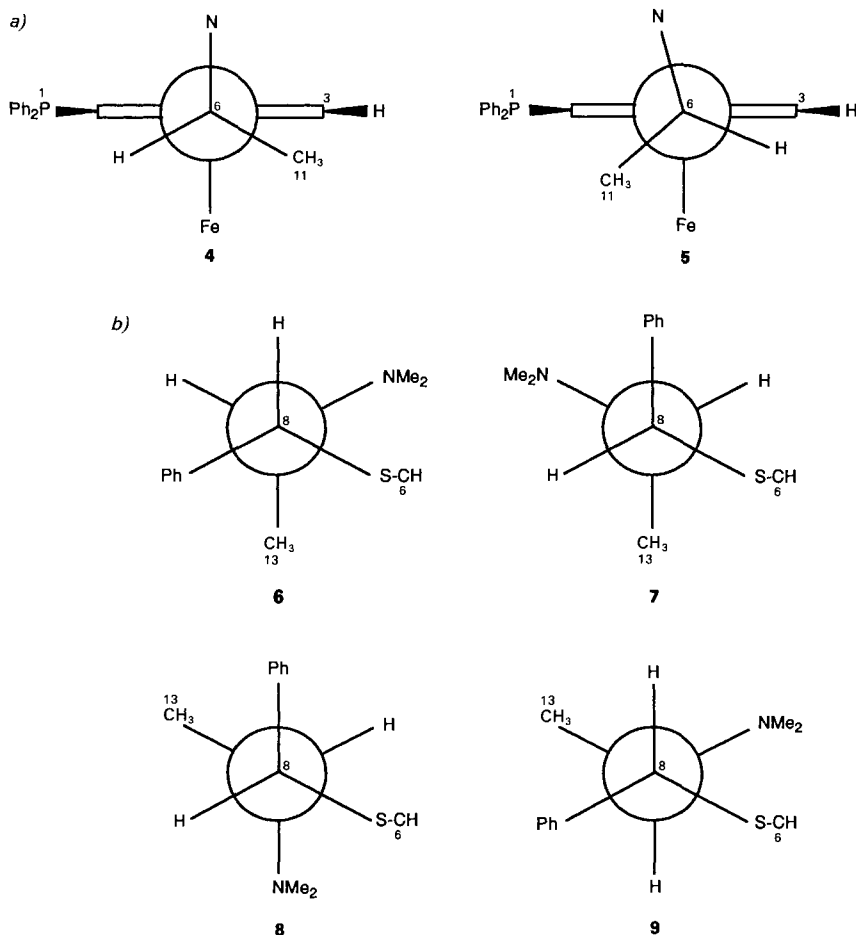


Fig. 3. Newman projections a) along the C(6)–C(2) bond of **4** and **5** and b) along the C(8)–C(9) bond of **6–9**: preferred conformations according to NOESY results

from obvious conformational differences, the side chain in ligands **6–9** all seem to be 'isolated' from the C(6)–ferrocenyl part, *i.e.* in the NOESY spectra, no cross-peaks of short contacts between the C(8)–C(9) fragment and the rest of the molecule are seen. However, the S–C(8)–C(9)–N moiety adopts different conformations in all four cases. The vicinal coupling constants $^3J(H-C(8), H-C(9))$ for **6–9** are 6.5, 8.8, 9.2, and 10.0 Hz, respectively. Given the known relationship between this parameter and the dihedral angle (*Karplus* equation [23]), one can conclude that these two protons are *synclinal* in **6**, whereas, in **7–9**, they are very likely *antiperiplanar*. The NOESY data confirm this by a substantial *H–C(8), H–C(9)* NOE only for **6**. In **8** and **9** there is a NOE between CH₃(13) and Ph–C(8), whereas this contact is absent in **6** and **7**. For all four compounds **6–9**, moderate Me₂N, *H–C(8)* NOE's were found. Finally, **7–9** show a *H–C(8), CH₃(13)* contact which is absent in **6**. These latter NOE's combined with the vicinal coupling constants are sufficient to define the overall conformations of the side chains (see Fig. 3).

An inspection of both the ¹H and ¹³C chemical shift data shows only routine values, with one exception: for **4** and **5** δ(C) of C(11) are rather different (9.8 and 16.5 ppm, resp.), and both values are different from the δ(C)'s of C(11) in **6–9** (*ca.* 22–23 ppm). C(11) in **4** might experience a γ-substituent effect [24]; we do not believe that the

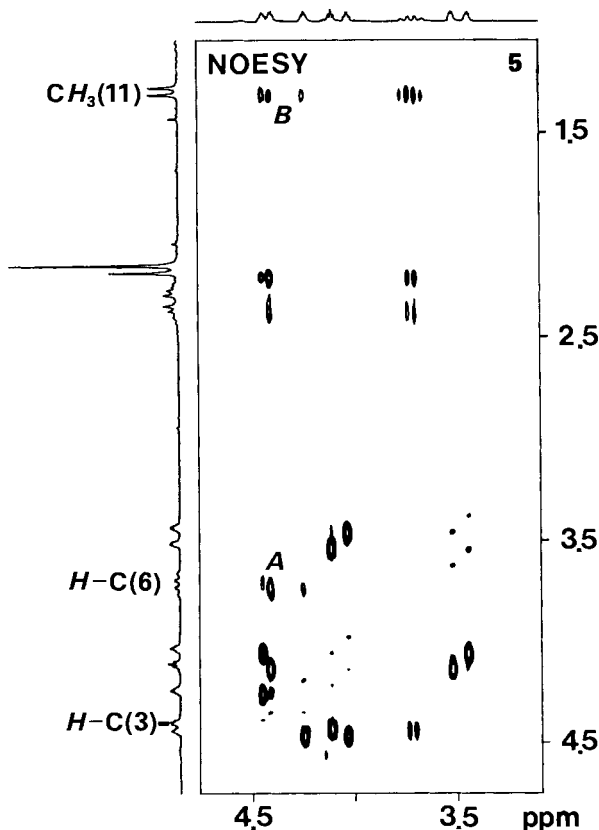


Fig. 4. Section of the NOESY spectrum (CDCl₃, 200.13 MHz) of **5**. Key cross-peaks are indicated: A, H-C(6) with Cp proton; B, CH₃(11) with several Cp protons.

ferrocenyl unit is responsible for this, since this $\delta(\text{C})$ appears at a relatively normal position in all other ligands.

Thus, one can use NOE's combined with classical coupling constants and some few chemical shifts, to define the conformation of the C(6)–C(11) unit with respect to the ferrocenyl moiety. The conformation of the remaining section of the side chain can also be elucidated; however, there seems to be no close contact between the two main fragments of the molecules.

2.3. Conformation of the Ligands and Stereoselectivity of the Gold(I)-Catalyzed Aldol Reaction. In the context of our study and in terms of the selectivity of the gold(I)-catalyzed aldol reaction, the most important structural feature of these ligands is the one related to the absolute configuration at C(6). This is reflected by the different NMR characteristics of **5**, as discussed above, paralleled by the profound alteration of the selectivity observed with this ligand. As shown in Fig. 3a, the dihedral angle C(1)–C(2)–C(6)–N is *ca.* 90° in both **4** and **5**, *i.e.* the position of this N-atom (and of the S-atom in **6–9**) remains relatively constant with respect to the ferrocenyl moiety and a modification of the configuration at C(6) corresponds *de facto* to an exchange of the

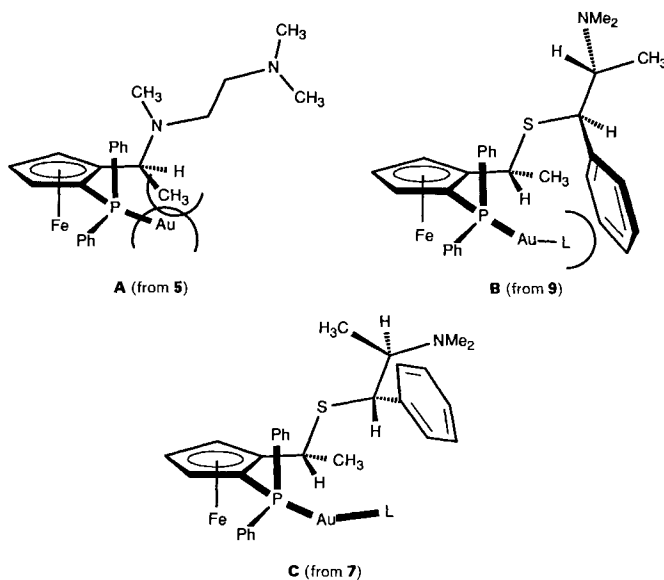


Fig. 5. Most probable detrimental interactions in the catalysts **A** and **B** formed from **5** and **9**, respectively, as compared to catalyst **C** from **7**. The lower Cp rings have been omitted for clarity; L = CNCH₂COOR.

mutual positions of H–C(6) and CH₃(11). Thus, CH₃(11) of **5** will very likely sterically interfere with the coordinated Au^I cation pushing it ‘down’ in the catalytically active complex (see **A** in Fig. 5). This, in turn will affect the position and orientation of the isocyanoenolate and its ability to interact with the pendant Me₂N group [21].

We noted above that no significant contacts exist between the C(8)–C(9) section and the rest of the molecule. We take this observation as an indication that the conformation of the ‘outer’ segment of the side chain is not interlocked with the one of the ferrocenyl–C(6) portion of the ligand. Furthermore, we suggest that the C(8)–C(9) fragment will affect the selectivity of the catalytic reaction in a way that can be dealt with independently.

It is apparent that the two ligands **6** and **9**, which give low selectivities, also have structurally common features (see Fig. 3b): 1) the Me₂N group is in synclinal position with respect to the S-atom and oriented toward the ‘backside’ of the side chain; 2) the relative positions of the S-atom, Ph–C(8), and Me₂N are identical in both ligands. The position of Ph–C(8) in **6/9** vs. **7/8** (due to the change in absolute configuration at C(8)) is an important aspect in trying to interpret the dramatic differences in selectivity observed. In the catalyst formed from **6** and **9**, Ph–C(8) is close to where the oxazoline-forming reaction is supposed to take place (see **B** in Fig. 5). Thus, the interference of Ph–C(8) with the coordinated enolate is likely to be the main factor responsible for low selectivity. Further, in **7** and **8** the Me₂N group is oriented toward the ‘front side’ of the side chain (see **C**), although its relative position is different in these two ligands (change in absolute configuration at C(9)).

It can now be concluded that the ligand giving high selectivities will most probably display substituents on the side chain which, because of their position, do not sterically

interact with the Au¹ cation or its further ligands. The same substituents will ensure a conformation such that the Me₂N group will be oriented in the direction of the coordinated enolate. In order to corroborate these ideas, ligands are currently being prepared which contain a side chain imbedded in a bicyclic system and which, therefore, display a rigid conformation similar to that of **7** and **8**.

The authors thank Dr. *Christian Ammann* and Dr. *Heinz Rügger* for NMR-technical assistance.

Experimental Part

Ligands 4, 5 [6], and *6–9* [12] were prepared as described previously.

NMR Spectroscopy. Samples in 5-mm tubes at r.t., prepared by degassing a soln. of 20 mg of ligand in CDCl₃ via the freeze-thaw method and then sealing the tube; standard *Bruker* software; δ in ppm rel. to TMS as internal standard for ¹H and ¹³C and to 85% H₃PO₄ soln. as external standard for ³¹P; 2D-NMR experiments without spinning; for ¹H-COSY and ¹H,¹³C- and ¹H,³¹P-HMQC spectra, standard pulse sequences were used [25].

2D Phase-Sensitive NOESY. The NOESY spectra resulted from a 256 × 1024 or 256 × 2048 data matrix size with 32 or 56 transients per *t*₁ value. The recycle delay time was 2.0 s and the mixing time was 1.0 s (200 MHz) and 0.8 s (500 MHz). The cross-peak intensities were qualitatively the same in both cases. Employing the TPPI method gave pure absorption-mode spectra. The spectra were obtained by multiplying the data with a cosine squared bell function in both dimensions and zero filling in the *F*₁ dimension before *Fourier* transformation. The digital resolution was always better than 2.5 Hz per point. *T*₁ measurements were performed to assist in the determination of the optimal mixing time. The *T*₁'s were measured using the standard inversion recovery technique. Different mixing times have been tested, e.g., 0.7, 1.0, and 1.3 s, for optimizing certain points of the spectra. The results of the 2D spectra were confirmed by NOE difference experiments on different magnetic fields, so at 200.13 and 300.13 MHz. A relaxation delay of 24 s and a NOE generation time of 2.0 s was chosen. The results were essentially the same for both magnetic fields. For **7**, the integrals of the NOE from CH₃(11) gave the following values (300.13 MHz): *H–C*(6) 8.2, *H–C*(8) 2.4, *H–C*(9) 5.9, *H–C*(3) 6.2, *H–C*(2') 3.7, and *H–C*(3') 3.1%.

REFERENCES

- [1] T. Hayashi, in 'Organic Synthesis: an Interdisciplinary Challenge', Eds. J. Streith, H. Prinzbach, and G. Schill, Blackwell, Oxford–London–Edinburgh–Boston–Melbourne, 1985, pp. 35–42.
- [2] T. Hayashi, *Pure Appl. Chem.* **1988**, *60*, 7.
- [3] T. Hayashi, M. Kumada, *Acc. Chem. Res.* **1982**, *15*, 395.
- [4] For a definition of this terminology, see K. Mislow, J. Siegel, *J. Am. Chem. Soc.* **1984**, *106*, 3319.
- [5] For examples of the various types of side chains adapted to the specific requirements of different catalytic reactions, see a) T. Hayashi, M. Konishi, M. Fukushima, T. Mise, M. Kagotani, M. Tajika, M. Kumada, *J. Am. Chem. Soc.* **1982**, *104*, 180; b) T. Hayashi, A. Katsumura, M. Konishi, M. Kumada, *Tetrahedron Lett.* **1979**, 425; c) T. Hayashi, A. Yamamoto, T. Hagihara, Y. Ito, *ibid.* **1986**, *27*, 191; d) T. Hayashi, Y. Matsumoto, I. Morikawa, Y. Ito, *Tetrahedron: Asymmetry* **1990**, *1*, 151.
- [6] T. Hayashi, T. Mise, M. Fukushima, M. Kagotani, N. Nagashima, Y. Hamada, A. Matsumoto, S. Kawakami, M. Konishi, K. Yamamoto, M. Kumada, *Bull. Chem. Soc. Jpn.* **1980**, *53*, 1138.
- [7] G. W. Gokel, D. Marquarding, I. K. Ugi, *J. Org. Chem.* **1972**, *37*, 3052.
- [8] D. Marquarding, H. Klusacek, G. Gokel, P. Hoffmann, I. Ugi, *J. Am. Chem. Soc.* **1970**, *92*, 5389.
- [9] Y. Ito, M. Sawamura, T. Hayashi, *J. Am. Chem. Soc.* **1986**, *108*, 6405; see also T. Hayashi, Y. Uozumi, A. Yamazaki, M. Sawamura, H. Hamashima, Y. Ito, *Tetrahedron Lett.* **1991**, *32*, 2799, and ref. cit. therein.
- [10] A. Togni, S. D. Pastor, *J. Org. Chem.* **1990**, *55*, 1649.
- [11] S. D. Pastor, A. Togni, *J. Am. Chem. Soc.* **1989**, *111*, 2333.
- [12] A. Togni, R. Häusel, *Synlett.* **1990**, 633.
- [13] A. Togni, S. D. Pastor, *Helv. Chim. Acta* **1989**, *72*, 1038.
- [14] A. Togni, S. D. Pastor, G. Rihs, *Helv. Chim. Acta* **1989**, *72*, 1471.

- [15] A. Togni, S.D. Pastor, G. Rihs, *J. Organomet. Chem.* **1990**, *381*, C21.
- [16] S.D. Pastor, A. Togni, *Helv. Chim. Acta* **1991**, *74*, 905.
- [17] A. Togni, S.D. Pastor, *Chirality* **1991**, *3*, in press.
- [18] S. Masamune, W. Choy, J. S. Petersen, L. R. Sita, *Angew. Chem. Int. Ed.* **1985**, *24*, 1.
- [19] A. Togni, G. Rihs, P.S. Pregosin, C. Ammann, *Helv. Chim. Acta* **1990**, *73*, 723.
- [20] H. Rügger, H. W. Kunz, C. Ammann, P.S. Pregosin, *Magn. Reson. Chem.* **1991**, *29*, 197.
- [21] M. Sawamura, Y. Ito, T. Hayashi, *Tetrahedron Lett.* **1990**, *31*, 2723.
- [22] J.G. Verkade, L.D. Quin, Eds., ³¹P-NMR Spectroscopy and Stereochemical Analysis', VCH Publishers, Deer Field Beach, Florida, 1987, Vol. 8.
- [23] F. A. Bovey, 'Nuclear Magnetic Resonance', Academic Press, New York, 1969.
- [24] H.-O. Kalinowski, S. Berger, S. Braun, ¹³C-NMR Spektroskopie', Thieme, Stuttgart, 1984.
- [25] H. Kessler, M. Gehrke, C. Griesinger, *Angew. Chem.* **1988**, *100*, 507; *ibid. Int. Ed.* **1988**, *27*, 490, and ref. cit. therein.